Available online at www.sciencedirect.com
ScienceDirect
International Journal of Pharmaceutics 351 (2008) 227–235
INTERNATIONAL JOURNAL OF PHARMACEUTICS
www.elsevier.com/locate/ijpharm

Chitosan–magnesium aluminum silicate composite dispersions: Characterization of rheology, flocculate size and zeta potential

Wanwisa Khunawattanakul [a], Satit Puttipipatkhachorn [b], Thomas Rades [c], Thaned Pongjanyakul [a,*]

[a] *Faculty of Pharmaceutical Sciences, Khon Kaen University, Khon Kaen 40002, Thailand*
[b] *Department of Manufacturing Pharmacy, Faculty of Pharmacy, Mahidol University, Bangkok 10400, Thailand*
[c] *School of Pharmacy, University of Otago, PO Box 913, Dunedin, New Zealand*

Received 4 June 2007; received in revised form 5 September 2007; accepted 30 September 2007
Available online 5 October 2007

Abstract

Composite dispersions of chitosan (CS), a positively charged polymer, and magnesium aluminum silicate (MAS), a negatively charged clay, were prepared and rheology, flocculate size and zeta potential of the CS–MAS dispersions were investigated. High and low molecular weights of CS (HCS and LCS, respectively) were used in this study. Moreover, the effects of heat treatment at 60 °C on the characteristics of the CS–MAS dispersions and the zeta potential of MAS upon addition of CS at different pHs were examined. Incorporation of MAS into CS dispersions caused an increase in viscosity and a shift of CS flow type from Newtonian to pseudoplastic flow with thixotropic properties. Heat treatment brought about a significant decrease in viscosity and hysteresis area of the composite dispersions. Microscopic studies showed that flocculation of MAS occurred after mixing with CS. The size and polydispersity index of the HCS–MAS flocculate were greater than those of the LCS–MAS flocculate. However, a narrower size distribution and the smaller size of the HCS–MAS flocculate were found after heating at 60 °C. Zeta potentials of the CS–MAS flocculates were positive and slightly increased with increasing MAS content. In the zeta potential studies, the negative charge of the MAS could be neutralized by the addition of CS. Increasing the pH and molecular weight of CS resulted in higher CS concentrations required to neutralize the charge of MAS. These findings suggest that the electrostatic interaction between CS and MAS caused a change in flow behavior and flocculation of the composite dispersions, depending on the molecular weight of CS. Heat treatment affected the rheological properties and the flocculate size of the composite dispersions. Moreover, pH of medium and molecular weight of CS influence the zeta potential of MAS.

Keywords: Chitosan; Magnesium aluminum silicate; Rheology; Flocculation; Zeta potential; Heat treatment

1. Introduction

Chitosan (CS), a deacetylated derivative of chitin, consists of D-glucosamine and *N*-acetyl-D-glucosamine units. CS is a weak base with a pK_a value of the D-glucosamine residues between 6.2 and 7.0 (Hejazi and Amiji, 2003). CS is thus insoluble at neutral and alkaline pH. In acidic medium however, CS is soluble as the amino groups of CS are protonated (Illum, 1998). CS has been widely used in pharmaceutical formulations due to its non-toxicity, biodegradability, and biocompatibility (Illum, 1998). In addition, chitosan has further advantages that make it particularity suitable for the development of drug delivery systems such as its mucoadhesive properties, which could prolong the resident time of delivery systems on the site of administration (Grabovac and Guggi, 2005), its permeation enhancing properties (Bernkop-Schnürch, 2000; Senel et al., 2000a), its film-forming ability (Senel et al., 2000b; Nunthanid et al., 2001), and its controlled release properties (Senel et al., 2000b; Giunchedi et al., 2002).

Magnesium aluminum silicate (MAS) is a mixture of natural smectite clays, in particular montmorillonites and saponites (Kibbe, 2000). It has a layer structure which is composed of tetrahedrally coordinated silica atoms fused into an edge-shaped octahedral plane of either aluminum hydroxide or magnesium hydroxide (Alexandre and Dubois, 2000; Kibbe, 2000). The layer structures of MAS can be separated when they are hydrated

* Corresponding author. Tel.: +66 43 362092; fax: +66 43 202379.
E-mail address: thaned@kku.ac.th (T. Pongjanyakul).

0378-5173/$ – see front matter © 2007 Elsevier B.V. All rights reserved.
doi:10.1016/j.ijpharm.2007.09.038

in water. Once MAS is hydrated, the weakly positively charged edges are attracted to the negatively charged faces of the colloidal layers of MAS. The attraction of face to edge of these colloidal layers creates a three dimensional colloidal structure throughout the dispersion, which exhibits thixotropic properties (Zatz and Kushla, 1989). Thus, MAS has been widely used in pharmaceutical development as a suspending and stabilizing agent (Kibbe, 2000). Moreover, the positively charged edges on the layers of MAS could interact with anionic polymers, such as xanthan gum (Ciullo, 1981), carbomer (Ciullo and Braun, 1991), and sodium alginate (Pongjanyakul et al., 2005), which resulted in viscosity synergism and increase in thixotropic properties of polymeric dispersions.

Several groups have reported the effects of polymers, such as polyvinyl alcohol (Chang et al., 1992), polyethylene glycol (Ece et al., 2002; Alemdar et al., 2005), and polyacrylamide (Güngör and Karaoglan, 2001) on the rheological properties of dispersion of montmorillonite clays, particularly bentonite. Moreover, clay particles were also found to form a flocculate due to a bridging mechanism with the polymer chain (Yoon and Deng, 2004). Recently, the rheological properties and zeta potential of natural bentonite–CS dispersions were studied by Günister et al. (2007). However, this study did not investigate a potential flocculation of clay upon the addition of CS.

Wang et al. (2005) have shown that CS and montmorillonite clay can form nanocomposite films, when CS–clay dispersions were prepared and treated at 60 °C, and then casted on plastic molds and dried at high temperature. Moreover, heat treatment on CS–montmorillonite dispersion has also been used to induce the formation of nanocomposites (Darder et al., 2003, 2005). However, there is no data available concerning the characteristics of CS–clay dispersions before casting, although it is likely that the characteristics of the composite dispersions will influence the physical properties of these films.

In this study we report for the first time about the occurrence of clay flocculation induced by CS. The aim of the present study was to investigate the rheological characteristics, flocculate size, and zeta potential of CS–MAS composite dispersions. The effect of heat treatment at 60 °C on the properties of the composite dispersions was also investigated. A low and high molecular weight CS (LCS and HCS, respectively) were used in this study. MAS was used as a water washed purified grade. Moreover, the zeta potential of MAS dispersion upon addition of different concentrations of LCS and HCS at various pHs was determined. The CS–MAS composite dispersion could be used as a film-forming material, suspending and gelling agents in pharmaceutical formulations.

2. Materials and methods

2.1. Materials

LCS (molecular weight of 200 kDa) and HCS (molecular weight of 800 kDa) with an 85% degree of deacetylation were purchased from Seafresh Chitosan (Lab) Co. Ltd. (Bangkok, Thailand). MAS (Veegum®HV) was obtained from R.T. Vanderbilt Company Inc. (Norwalk, CT, USA). All other reagents used were of analytical grade and used as received.

2.2. Preparation of dispersions

CS colloidal solutions (1% w/v) in 1% acetic acid were prepared by stirring overnight at room temperature. MAS fine suspensions (4% w/v) were prepared by using hot water and adjusting to the final volume using distilled water. Then, the 4% (w/v) MAS suspensions were diluted using 10 mM acetate buffer at pH 4 to achieve the final 1% (w/v) MAS dispersion. After that, 50 ml of the 1% (w/v) chitosan solution were added into 0, 10, 30, and 50 ml of the 1% (w/v) MAS dispersion and adjusted to the final pH of 4 by using glacial acetic acid and the final volume using 10 mM acetate buffer at pH 4 to achieve the final concentration 0.5% (w/v) chitosan with 0, 0.1, 0.3, and 0.5% (w/v) MAS, respectively. The dispersions were mixed for 1 min using a homogenizer and stored at room temperature for 24 h before testing.

To investigate the effect of heat treatment, the dispersions were prepared using the methods described above and incubating at 60 °C for 48 h prior to testing.

The effect of CS addition on the zeta potential of MAS dispersions was studied by adding 0–3.5 ml of a 10 $\mu g\,ml^{-1}$ CS colloidal solution into a 10 ml test tube which had been filled with 0.5 ml of a 1000 $\mu g\,ml^{-1}$ MAS dispersion and adjusted to 5 ml using 10 mM acetate buffer at pH 3.0 ± 0.2, 4.0 ± 0.2, or 6.0 ± 0.2. Hence, MAS dispersions of 100 $\mu g\,ml^{-1}$ with 0–7 $\mu g\,ml^{-1}$ of CS were obtained. All dispersions were vortexed for 15 s and the zeta potential of the dispersion was immediately measured.

The effect of MAS addition on the zeta potential of CS colloidal solutions was studied by adding 0.5 ml of a 1000 $\mu g\,ml^{-1}$ CS colloidal solution into a 10 ml test tube, which had been filled with 0–0.5 ml of a 1000 $\mu g\,ml^{-1}$ MAS dispersion, and adjusted to 5 ml by using 10 mM acetate buffer at pH 4.0 ± 0.2. CS colloidal solutions (100 $\mu g\,ml^{-1}$) with 0–100 $\mu g\ ml^{-1}$ of MAS were obtained. All dispersions were vortexed for 15 s and the zeta potential of the dispersion was immediately measured.

2.3. Microscopic morphology studies

The morphology of the MAS particles and CS–MAS flocculates in dispersion were investigated using a inverted microscope (Eclipse TS100, Nikon, Japan) and examined by using a digital camera (Coolpix 4500, Nikon, Japan).

2.4. Rheological studies

The rheological properties of the dispersions were studied by using a Brookfield digital rheometer (Model DV-III, Brookfield Engineering Laboratories Inc., Middleboro, MA, USA). The temperature of all samples was controlled at 33 ± 1 °C. A rheogram of the samples was plotted using shear rate and shear stress at various revolution rates of the spindle (SC4-34). The area of the hysteresis loop of the rheogram was computed from the difference between the area under the up-curve and

the down-curve by using the trapezoidal rule. Moreover, other rheological parameters of the dispersions were calculated using the following equations (Martin, 1993):

$$F^{N} = \eta G \quad (1)$$

$$\log G = N \log F - \log \eta \quad (2)$$

where G, F, N and η are shear rate, shear stress, exponential constant that defines the type of flow, and viscosity coefficient, respectively.

2.5. Particle size determination

The particle size of the MAS dispersions and of the dispersed phase of the composite dispersions was measured using a laser diffraction particle size analyzer (Mastersizer2000 Model Hydro2000SM, Malvern Instrument Ltd., UK). The samples were dispersed in 70 ml of 10 mM acetate buffer at pH 4 in a small volume sample dispersion unit and stirred at a rate of 50 Hz for 30 s before the measurement. The size-frequency distributions were plotted and $D_{10\%}$, $D_{50\%}$, and $D_{90\%}$, volume number diameters where the indicated percentage of the particles is smaller than that size, were determined. In addition, the size distribution was computed in terms of the polydispersity index (PI) and expressed as (Torrado et al., 1989):

$$\mathrm{PI} = \frac{D_{90\%} - D_{10\%}}{D_{50\%}} \quad (3)$$

2.6. Zeta potential measurement

The zeta potential of all samples was measured by using a laser Doppler electrophoresis analyzer (Zetasizer Model ZEN 2600, Malvern Instrument Ltd., UK). The temperature of the samples was controlled at 25 °C. The MAS and CS–MAS dispersions were diluted to obtain appropriate concentrations (count rates >20,000 counts/s) prior to the measurement.

2.7. Statistical analysis

One-way analysis of variance (ANOVA) with the least significant difference (LSD) test for multiple comparisons and Student's *t*-test were performed using the software SPSS for MS Windows, release 11.5 (SPSS Inc., Chicago, IL) to assess statistical significance of the effect of the MAS concentration and the heat treatment on the flocculate size, respectively. The significance of the difference was determined at 95% confident limit ($\alpha = 0.5$) and considered to be significant at a level of P less than 0.05.

3. Results and discussion

3.1. Appearance of composite dispersions

Whilst the colloidal CS dispersions were transparent liquids, the particulate MAS dispersions were opaque in nature (Fig. 1). Sedimentation of the dispersed phase of the CS–MAS dispersions was faster than that of the particles in the MAS dispersion as shown in Fig. 1. This suggested that the particle size of the dispersed phase of the MAS dispersion increased when mixed with CS. Furthermore, 0.5% LCS with 0.1% MAS showed the fastest sedimentation rate of dispersed phase. According to Stokes' law, this is likely to be due to the lower viscosity of this dispersion.

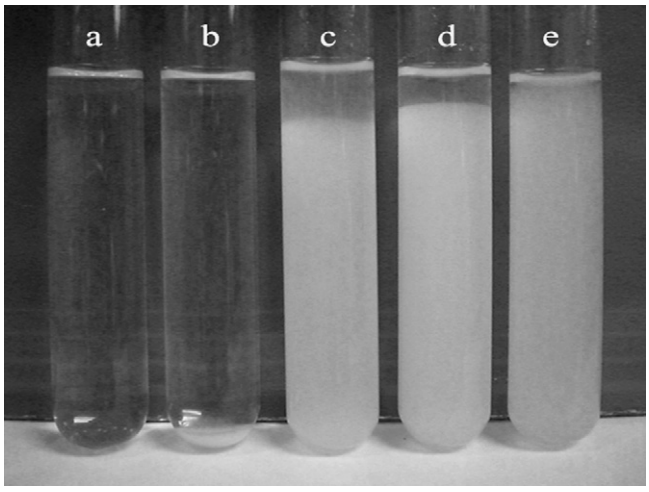

Fig. 1. Photograph of 0.5% LCS dispersions containing 0% (a), 0.1% (b), 0.3% (c) and 0.5% (d) MAS, and 0.5% MAS dispersion (e) after settling for 2 h.

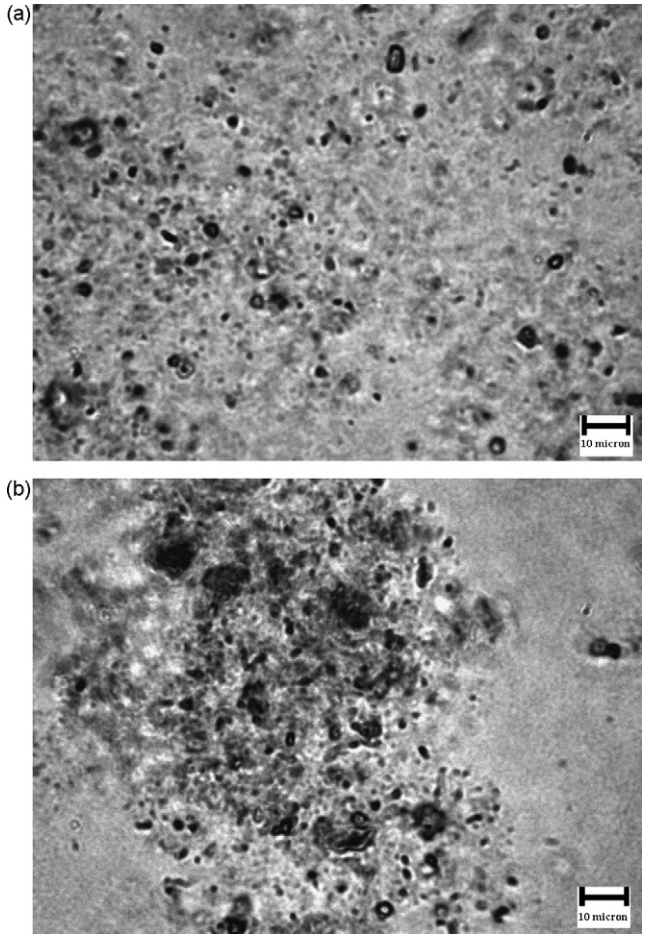

Fig. 2. Micrographs of MAS particles in a 0.5% MAS dispersion (a) and in a 0.5% LCS dispersion containing 0.5% MAS (b).

In addition, the supernatant liquid of the LCS–MAS dispersions was clear, suggesting a flocculated system. The microscopic morphology of 0.5% MAS dispersion showed separated particles of hydrated MAS (Fig. 2a), whereas flocculation of MAS particles in 0.5% LCS dispersion could be observed (Fig. 2b). This is likely to be due to electrostatic interactions between the negatively charged silanol groups ($-SiO^-$) on the silicate layers of MAS and the positively charged amino groups ($-NH_3^+$) of CS, causing a change in particle size of the dispersed phase, which

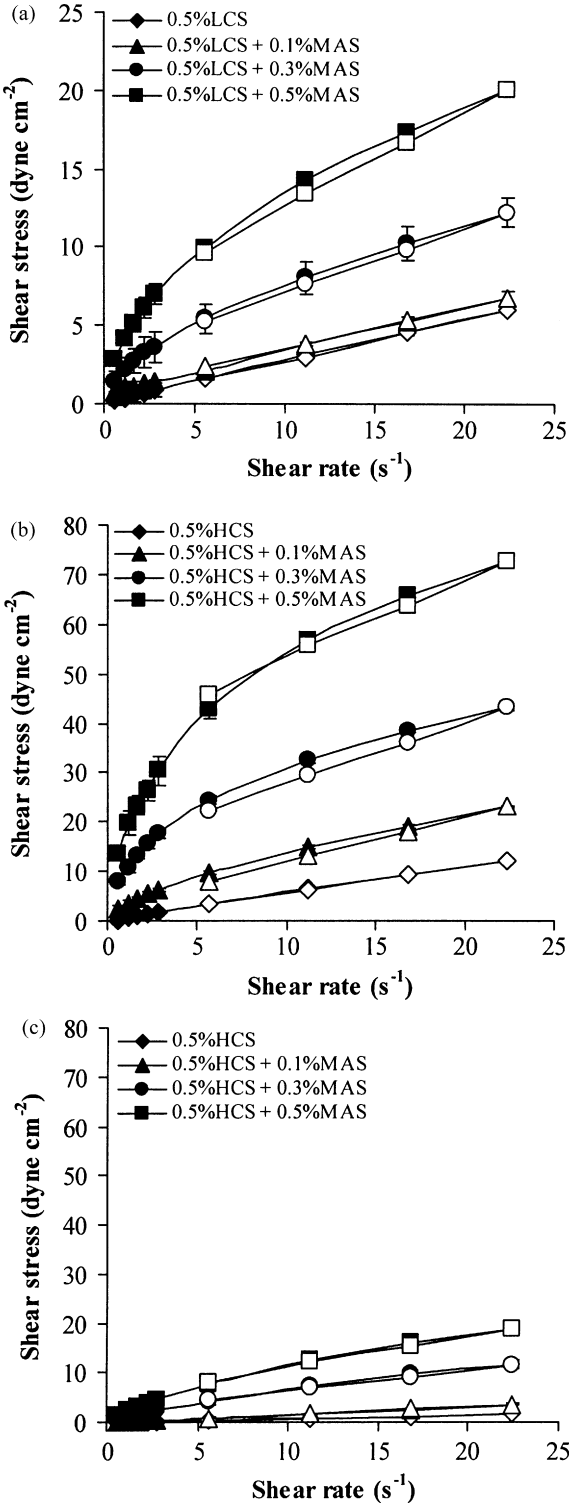

Fig. 3. Rheograms of CS–MAS dispersions prepared using 0.5% LCS added various concentrations of MAS without heat treatment (a), and 0.5% HCS added various concentrations of MAS without (b) and with heat treatment (c). Closed symbols represent the up-curve; open symbols represent the down-curve. Each point is the mean ± S.D. of three determinations.

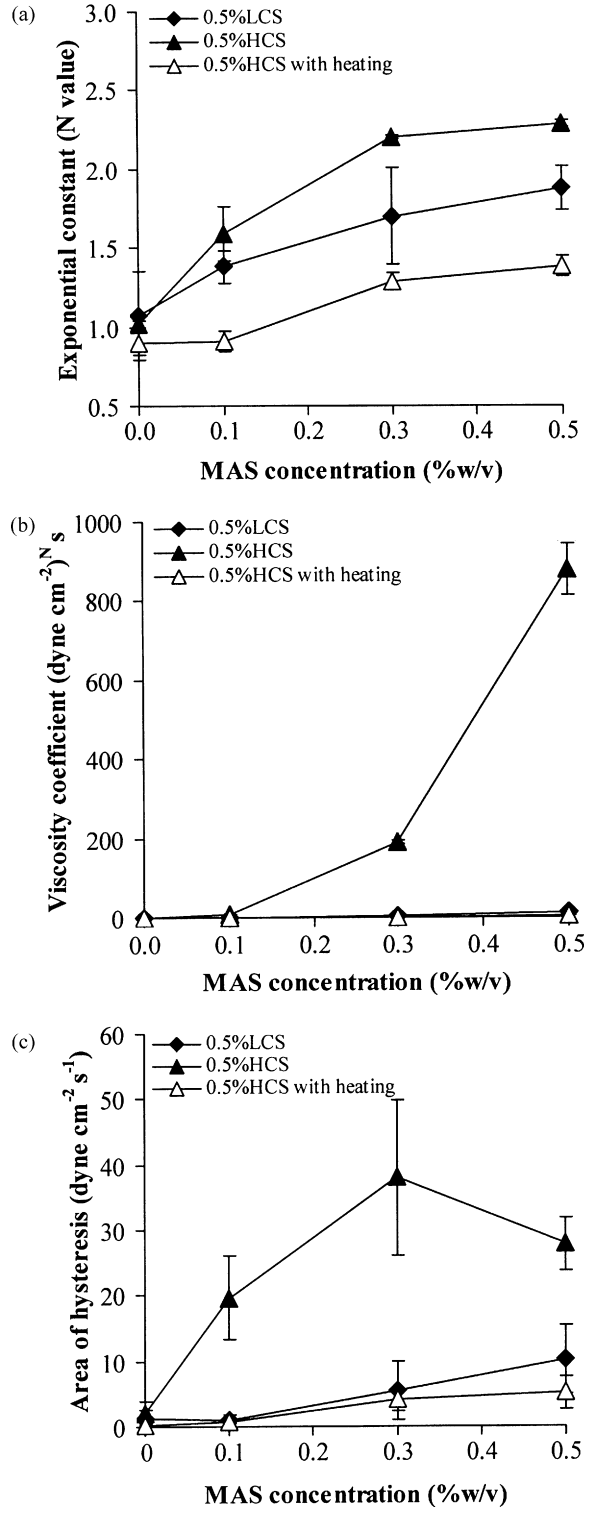

Fig. 4. Exponential constant (*N* value) (a), viscosity coefficient (b), and area of hysteresis (c) of CS–MAS dispersions. Each point is the mean ± S.D. of three determinations.

may affect zeta potential and flow behavior of the composite dispersion.

3.2. Characteristics of CS–MAS composite dispersions

The effect of MAS addition on the flow curve of LCS and HCS dispersions is shown in Fig. 3a and b, respectively. Non-linear flow curves of the composite dispersions were observed and the up- and down curves of the composite dispersions did not coincide in contrasts to the flow curves of pure CS dispersions. The rheological parameters calculated using shear rate and shear stress of the up-curve are presented in Fig. 4. The exponential constant (N value), that defines the type of flow, of the CS dispersion was approximately unity (Fig. 4a), indicating Newtonian flow. Incorporating MAS into the CS dispersions caused an increase in the N value, suggesting that the flow behavior shifted to pseudoplastic flow. Moreover, the HCS–MAS dispersions showed higher N values than the LCS–MAS dispersions. The viscosity coefficient of the CS dispersion increased with increasing concentration of MAS (Fig. 4b), suggesting viscosity enhancing properties of MAS. The important parameter of the flow behavior of the composite dispersion was the hysteresis area between the up- and down parts of the flow curve as shown in Fig. 4c. Increasing hysteresis areas of the composite dispersion were found when MAS was added, indicative of an increase in thixotropic properties of the dispersions (Martin, 1993; Pongjanyakul et al., 2005). Heat treatment also affected the flow behavior. The flow curve of the LCS–MAS dispersion could not be obtained due to its very low viscosity. The HCS–MAS dispersions with heat treatment showed pseudoplastic flow (Fig. 3c), but the N value was smaller when compared with the composite dispersion without heat treatment (Fig. 4a). Moreover, heat treatment also caused a decrease of viscosity coefficient and hysteresis area of the HCS–MAS dispersion (Fig. 4b and c).

The size-frequency distributions of the CS–MAS flocculates of the composite dispersion with and without heat treatment are presented in Fig. 5. $D_{50\%}$ and PI of all dispersions are shown in Table 1. It can be seen that the flocculate size of the composite dispersions was significantly greater ($P<0.05$) than for the MAS dispersion. The LCS–MAS flocculates had a statistically smaller size ($P<0.05$) than the HCS–MAS flocculates at the same concentration of MAS, but a wider size of distribution was obtained from the HCS–MAS flocculates. An increase in MAS concentration of 0.1–0.5% gave a significantly greater flocculate size ($P<0.05$) of LCS, but did not affect the flocculate size of HCS when added 0.3–0.5% MAS. Heat treatment caused a significant decrease ($P<0.05$) in the flocculate size and PI values of LCS– and HCS–MAS dispersions. The CS–MAS flocculates showed a positive charge (zeta potential) when using both LCS and HCS. Surprisingly, the zeta potential of the flocculates increased slightly when MAS concentration in the dispersion was increased. However, heat treatment did not obviously influence the zeta potential of the flocculates.

Interaction between CS and MAS can immediately occur at pH 4. Between the negative charge of MAS and the positive

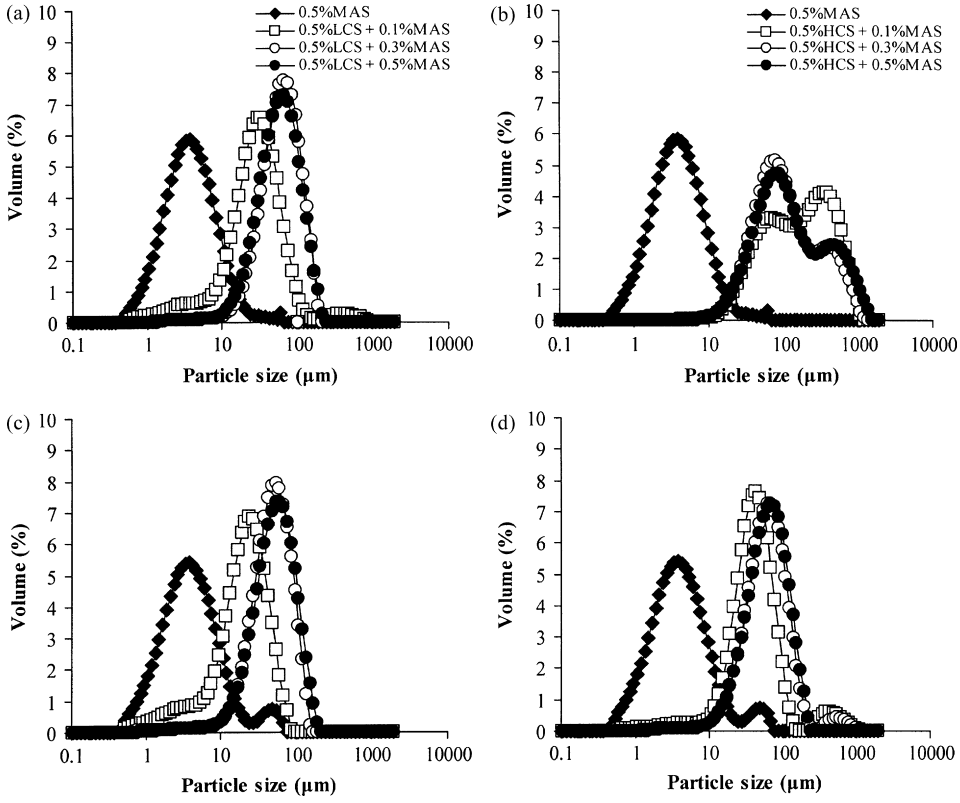

Fig. 5. Size-frequency distribution of LCS–MAS (a and c) and HCS–MAS (b and d) flocculates in composite dispersions without (a and b) and with (c and d) heat treatment.

Table 1
Particle size, polydispersity index, and zeta potential of CS, MAS and CS–MAS dispersions with and without heat treatment

Component	$D_{50\%}$[a] (μm)		Polydispersity index[a]		Zeta potential[b] (mV)	
	No heat treatment	Heat treatment	No heat treatment	Heat treatment	No heat treatment	Heat treatment
0.5% (w/v) MAS	3.67 ± 0.03	3.79 ± 0.01	2.38 ± 0.16	2.77 ± 0.06	−29.7 ± 0.9	−30.9 ± 1.4
0.5% (w/v) LCS	–	–	–	–	52.8 ± 5.2	46.7 ± 3.0
0.5% (w/v) LCS + 0.1% (w/v) MAS	26.3 ± 0.7	21.4 ± 0.8	2.16 ± 0.13	1.91 ± 0.01	57.9 ± 3.7	51.8 ± 3.3
0.5% (w/v) LCS + 0.3% (w/v) MAS	54.2 ± 0.9	49.3 ± 1.6	1.53 ± 0.01	1.51 ± 0.01	62.1 ± 0.6	58.8 ± 0.8
0.5% (w/v) LCS + 0.5% (w/v) MAS	59.2 ± 0.9	53.5 ± 1.5	1.68 ± 0.01	1.66 ± 0.01	63.2 ± 1.6	61.2 ± 1.0
0.5% (w/v) HCS	–	–	–	–	44.0 ± 8.9	41.6 ± 4.4
0.5% (w/v) HCS + 0.1% (w/v) MAS	158.0 ± 3.6	41.6 ± 1.7	3.22 ± 0.11	1.75 ± 0.14	57.1 ± 4.7	59.4 ± 1.5
0.5% (w/v) HCS + 0.3% (w/v) MAS	96.9 ± 4.6	60.8 ± 1.7	4.58 ± 0.25	1.79 ± 0.05	57.8 ± 2.9	55.9 ± 9.8
0.5% (w/v) HCS + 0.5% (w/v) MAS	99.6 ± 9.5	59.7 ± 1.5	4.97 ± 0.41	1.66 ± 0.01	62.8 ± 1.9	61.9 ± 1.8

–: Could not be measured.
[a] Data are the mean ± S.D. of three determinations.
[b] Data are the mean ± S.D. of six determinations.

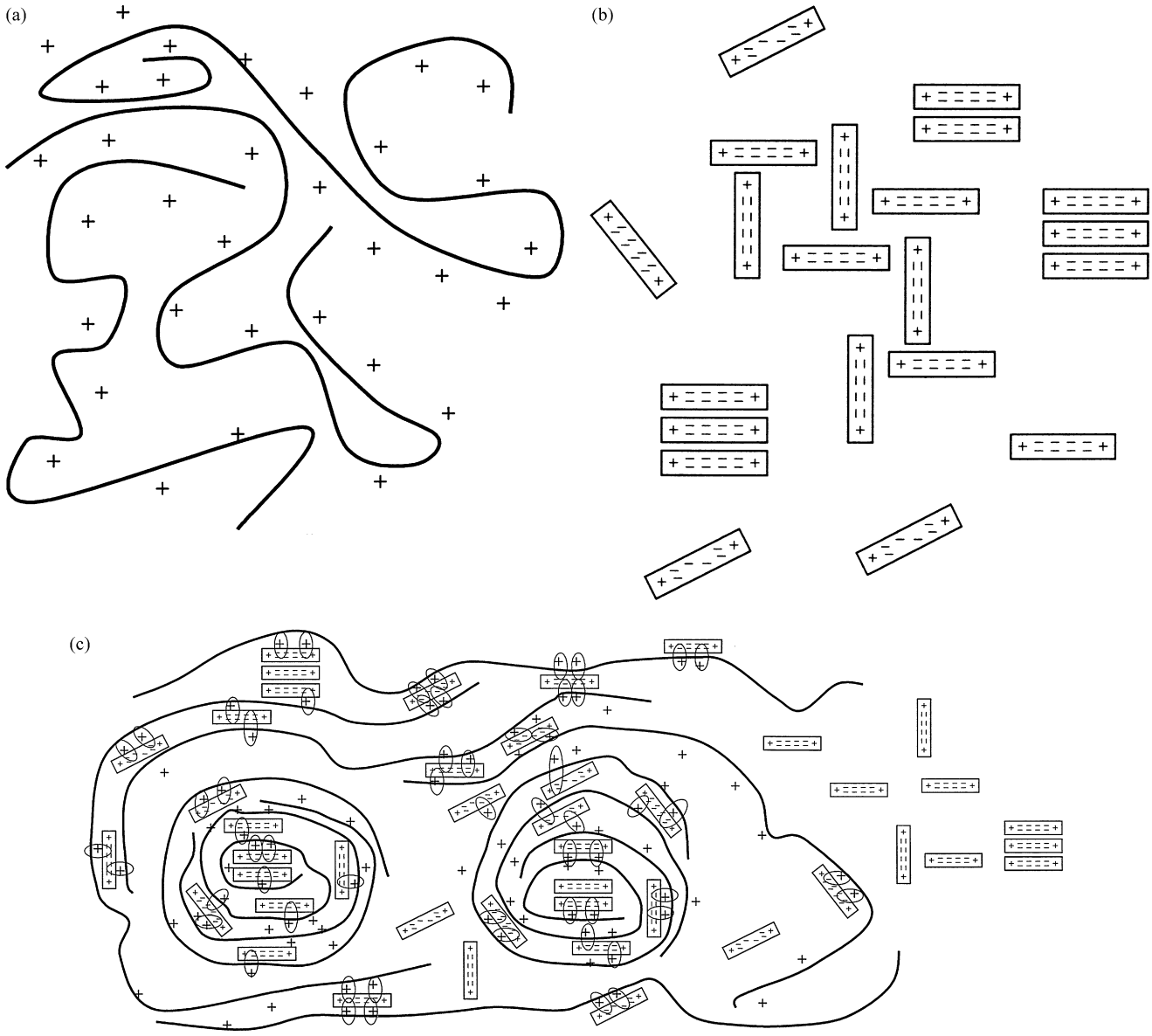

Fig. 6. Schematic models of CS (a), MAS (b), and CS–MAS composite dispersions.

charge of CS an electrostatic interaction can occur. This results in the flocculation of MAS induced by CS, with the CS–MAS flocculate size being significantly larger than the MAS size. The molecule weight of CS influenced the flocculation of MAS. The longer chain of the HCS could induce larger-sized flocculates. Moreover, the higher viscosity of HCS caused an obstacle to form denser and smaller-sized flocculates, which at least in part resulted in wider size distribution. This factor also influenced the flocculate size when increasing the concentration of MAS in the HCS dispersion. The zeta potential of the CS–MAS flocculate was positive, indicating that CS–MAS flocculates were covered by ionized CS molecules. The zeta potential of the flocculates increased slightly when the MAS concentration in the dispersions was increased possibly because a higher amount of CS molecules may be involved in the flocculation. This led to a higher positive charge density on the flocculate surface. From these results, a possible model for the CS–MAS flocculate is shown in Fig. 6. However, not all of the MAS molecules interacted with CS molecules to form the flocculates. Some silicate layers of MAS could act as a cross-linker between CS chains (Fig. 6c). This led to the formation of numerous points of contact and a loose three-dimensional network was created throughout the composite dispersion which was gel-like structure. The higher the content of MAS, the greater the number of points of contact in the dispersion, resulting in enhancement of viscosity and thixotropic properties of the composite dispersions. These results are similar to the effects of MAS on the rheology of sodium alginate and poloxamer 407 dispersions (Pongjanyakul et al., 2005). The composite dispersion underwent a gel-to-sol transformation and exhibited shear thinning when shear stress was applied. The structure started to reform slowly to the original state after the shear stress was removed.

The effect of heat treatment on the characteristics of the composite dispersion was also investigated in this study. The viscosity of the composite dispersion decreased remarkably after heating, causing a very low viscosity of the LCS–MAS dispersions (which in fact could not be measured with the rheological set up used in these experiments). However, the flow of the HCS–MAS dispersion with heat treatment still was pseudoplastic with thixotropic properties. The decrease in viscosity of the composite dispersion might be caused by a reduction of intramolecular hydrogen bonding of CS and a decrease in hydrogen-bonded hydration of CS (Chen and Tsaih, 1998), whereas heating did not affect the hydration of MAS because MAS dispersions were prepared and hydrated using hot water in the preparation process. In addition, heat treatment also affected the HCS–MAS flocculate size in the dispersion. This was likely to be due to the decrease in viscosity resulting in a flexibility of HCS at high temperature (Chen and Tsaih, 1998). This in turn meant that the HCS–MAS flocculates could be rearranged and denser structure were formed during heat treatment. Thus, a smaller size and narrower size distribution of the flocculates were obtained.

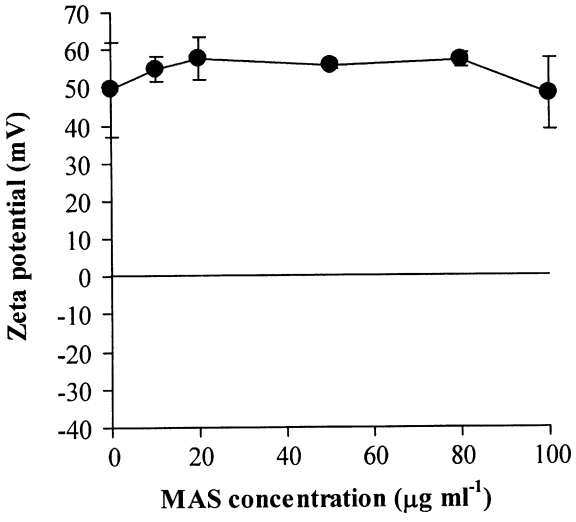

Fig. 7. Effect of MAS on the zeta potential of LCS colloidal solutions in pH 4 acetate buffer. Each point is the mean ± S.D. of six determinations.

3.3. Zeta potential studies

The effect of MAS addition on the zeta potential of LCS colloidal solutions in pH 4 acetate buffer is shown in Fig. 7. The zeta potential of the LCS colloidal solution was approximately +50 mV. Addition of MAS into the LCS colloidal solution did not affect zeta potential of LCS, even in the highest concentration of MAS (100 μg ml^{-1}) used. This result was in agreement with a previous study of Günister et al. (2007) that bentonite could not neutralize the zeta potential of CS even though the concentration of bentonite was 50-fold higher than CS. However, no clear explanations for this finding have been reported. The current data also indicates that MAS could not neutralize the positive charge of LCS. The possible reason for this surprising finding may be that LCS is a long chain molecule when compared with the silicate layers of MAS. The LCS–MAS flocculates were rapidly formed and the flocculates may be covered by LCS, resulting in a positively charged surface of the flocculates, independent of the MAS concentration.

On the other hand, LCS and HCS could gradually neutralize the negative charge of the silicate layers of MAS (Fig. 8). Moreover, the pH of the medium also affected the zeta potential of the MAS dispersion. This was due to the different ionization levels of CS and MAS at different pHs. The lower the pH of medium, the smaller the zeta potential of MAS because hydronium ions enriched in low pH medium could adsorb on the surface of the silicate layers, resulting in a decrease of the zeta potential of MAS (Fig. 8). In contrast, the lower pH medium caused higher ionization of the amino groups of CS, leading to a higher zeta potential of CS. Thus, it can be seen that the concentration, which could neutralize the zeta potential of MAS to zero (C_z), of LCS and HCS at pH 3 was lower than those at higher pHs (Fig. 9). The C_z values of LCS were comparable to those of HCS in pH 3 and 4, whereas the C_z value of LCS was obviously lower than that of HCS at pH 6. It is likely that the longer chain molecules of HCS caused a steric hindrance to completely adsorb on the surface of the silicate layers when compared with the short chain molecule of LCS. This led to a higher concentration of HCS necessary to neutralize the zeta potential of MAS.

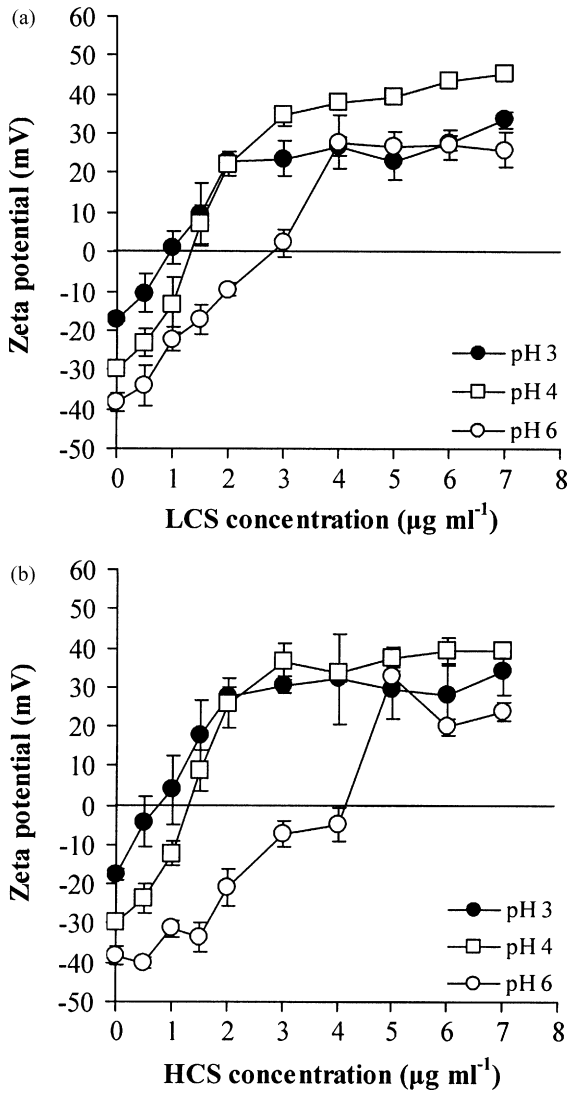

Fig. 8. Effect of LCS (a) and HCS (b) on the zeta potential of MAS dispersions in acetate buffer at different pHs. Each point is the mean ± S.D. of six determinations.

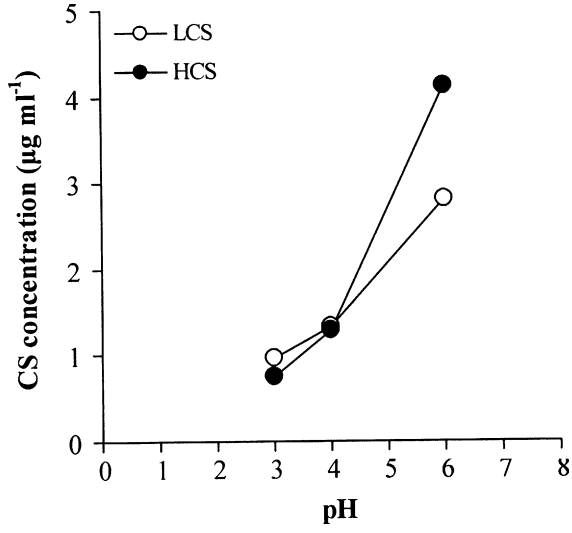

Fig. 9. CS concentration required to neutralize the zeta potential of MAS to zero at various pHs of the dispersion medium.

4. Conclusions

Electrostatic interaction between CS and MAS resulted in flocculate formation and caused a change in flow behavior, zeta potential and flocculate size of the composite dispersions. Heat treatment also affected viscosity and thixotropic properties, and flocculate size of the composite dispersions. Different zeta potentials upon addition of CS to MAS dispersions were found, in which the zeta potential was dependent upon the pH of the medium and the molecular weight of CS. This study indicates that the CS–MAS composite dispersions show differences in their rheological behavior, flocculate sizes and zeta potential characteristics, depending on CS molecular weight and heat treatment. This finding also indicated that the CS–MAS composite dispersions which showed a pseudoplastic flow with thixotropy may be applied as suspending and gelling agents in pharmaceutical products. Moreover, the CS–MAS flocculates formed may have a potential to entrap a drug and in situ formation of a drug delivery system, which however, remains to be shown in further investigations.

Acknowledgements

The authors wish to thank the Postgraduate Education Development (PED) for the development of higher education in Thailand based on Commission on Higher Education for research funding and the Faculty of Pharmaceutical Sciences, Khon Kaen Univeristy, Khon Kaen, Thailand, for technical support. Financial support from the Thailand Research Fund through the Royal Golden Jubilee Ph.D. Program (Grant No. PHD/0011/2549) for W. Khunawattanakul and T. Pongjanyakul is gratefully acknowledged.

References

Alemdar, A., Güngör, N., Ece, Ö.I., Atıcı, O., 2005. The rheological properties and characterization of bentonite dispersions in the presence of non-ionic polymer PEG. J. Mater. Sci. 40, 171–177.

Alexandre, M., Dubois, P., 2000. Polymer-layered silicate nanocomposites: preparation, properties and uses of a new class of materials. Mater. Sci. Eng. 28, 1–63.

Bernkop-Schnürch, A., 2000. Chitosan and its derivatives: potential excipients for peroral peptide delivery systems. Int. J. Pharm. 194, 1–13.

Chang, S.H., Gupta, R.K., Ryan, M.E., 1992. Effect of the adsorption of polyvinyl alcohol on the rheology and stability of clay suspensions. J. Rheol. 36, 273–287.

Chen, R.H., Tsaih, M.L., 1998. Effect of temperature on the intrinsic viscosity and conformation of chitosans in dilute HCl solution. Int. J. Biol. Macromol. 23, 135–141.

Ciullo, P.A., 1981. Rheological properties of magnesium aluminum silicate/xanthan gum dispersions. J. Soc. Cosmet. Chem. 32, 275–285.

Ciullo, P.A., Braun, D.B., 1991. Clay/carbomer mixtures enhance emulsion stability. Cosmet. Toilet. 106, 89–95.

Darder, M., Colilla, M., Ruiz-Hitzky, E., 2003. Biopolymer–clay nanocomposites based on chitosan intercalated in montmorillonite. Chem. Mater. 15, 3774–3780.

Darder, M., Colilla, M., Ruiz-Hitzky, E., 2005. Chitosan–clay nanocomposites: application as electrochemical sensors. Appl. Clay Sci. 28, 199–208.

Ece, Ö.I., Alemdar, A., Güngör, N., Hayashi, S., 2002. Influences of non-ionic poly(ethylene glycol) polymer PEG on electrokinetic and rheological properties of bentonite suspensions. J. Appl. Polym. Sci. 86, 341–346.

Giunchedi, P., Juliano, C., Gavini, E., Cossu, M., Sorrenti, M., 2002. Formulation and in vivo evaluation of chlorhexidine buccal tablets prepared using drug loaded chitosan microspheres. Eur. J. Pharm. Biopharm. 53, 233–239.

Grabovac, V., Guggi, D., Bernkop-Schnürch, A., 2005. Comparison of mucoadhesive properties of various polymers. Adv. Drug Deliv. Rev. 57, 1713–1723.

Güngör, N., Karaoglan, S., 2001. Interactions of polyacrylamide polymer with bentonite in aqueous systems. Mater. Lett. 48, 168–175.

Günister, E., Pestreli, D., Ünlü, C.H., Atıcı, O., Güngör, N., 2007. Synthesis and characterization of chitosan–MMT biocomposite systems. Carbohydr. Polym. 67, 358–365.

Hejazi, A., Amiji, M., 2003. Chitosan-based gastrointestinal delivery systems. J. Control. Release 89, 151–165.

Illum, L., 1998. Chitosan and its use as a pharmaceutical excipient. Pharm. Res. 15, 1326–1331.

Kibbe, H.A., 2000. Handbook of Pharmaceutical Excipients, 3rd ed. American Pharmaceutical Association, Washington, pp. 295–298.

Martin, A., 1993. Physical Pharmacy, 4th ed. Lea & Febiger, Philadelphia, pp. 453–476.

Nunthanid, J., Puttipipatkhachorn, S., Yamamoto, K., Peck, G.E., 2001. Physical properties and molecular behavior of chitosan films. Drug Dev. Ind. Pharm. 27, 143–157.

Pongjanyakul, T., Priprem, A., Puttipipatkhachorn, S., 2005. Influence of magnesium aluminium silicate on rheological, release and permeation characteristics of diclofenac sodium aqueous gels in-vitro. J. Pharm. Pharmacol. 57, 429–434.

Senel, S., İkinci, G., Kaş, S., Yousefi-Rad, A., Sargon, M.F., Hincal, A.A., 2000b. Chitosan films and hydrogels of chlorhexidine gluconate for oral mucosal delivery. Int. J. Pharm. 193, 197–203.

Senel, S., Kremer, M.J., Kaş, S., Wertz, P.W., Hincal, A.A., Squier, C.A., 2000a. Enhancing effect of chitosan on peptide drug delivery across buccal mucosa. Biomaterials 21, 2067–2071.

Torrado, J.J., Illum, L., Davis, S.S., 1989. Particle size and size distribution of albumin microspheres produced by heat and chemical stabilization. Int. J. Pharm. 51, 85–93.

Wang, S.F., Shen, L., Tong, Y.J., Chen, L., Phang, I.Y., Lim, P.Q., Liu, T.X., 2005. Biopolymer chitosan/montmorillonite nanocomposites: preparation and characterization. Polym. Degrad. Polym. 90, 123–131.

Yoon, S.Y., Deng, Y., 2004. Flocculation and reflocculation of clay suspension by different polymer systems under turbulent conditions. J. Colloid Interf. Sci. 278, 139–145.

Zatz, J.L., Kushla, G.P., 1989. Gels. In: Lieberman, H.A., Rieger, M.M., Banker, G.S. (Eds.), Pharmaceutical Dosage Forms: Disperse Systems, vol. 19. Marcel Dekker Inc., New York, pp. 495–510.